International Journal of GEOMATE
(Geotechnique, Construction Materials and Environment)
ISSN: 2186-2982 (P), 2186-2990 (O), Japan

Vol. 31, Issue 143, July, 2026, pp.106-116; DOI: 10.21660/2026.143.5405

CONVOLUTIONAL NEURAL NETWORK-BASED SPACE DETECTION MODEL FOR STIRRUPS AND TIES

*Samuel John Pajarillaga Abella[1], Donald Jasper Alcantara[1] and Christ John Lopez Marcos[1]

[1]School of Civil, Environmental, and Geological Engineering Department, Mapua University, Philippines

*Corresponding Authors, Received: 24 Dec. 2025, Revised: 27 Feb. 2026, Accepted: 10 Mar. 2026

ABSTRACT: Stirrup and tie inspection is tedious, especially in large-scale construction projects, which could bring problems in the balance of the Iron Triangle: time, cost, and quality management. This tedious inspection process could be optimized by applying recent advancements in deep-learning algorithms, specifically neural networks, in engineering. In this study, the training program and object detection technology used were MATLAB and YOLOv2, respectively. The dataset was primarily obtained from a physical model setup, comprising an equal number of images for beams and columns. Furthermore, dataset splitting was applied to the total of 2,142 images generated post-augmentation, using a 70-15-15 split for the training, validation, and test sets. After performing centroid location and distance calculations in MATLAB, the model was evaluated using multiple regression analysis and ANOVA to analyze the relationship between the dependent variables: spacing accuracy and average precision, and the independent variables: dataset size, learning rate, and image resolution. Based on the findings, a larger dataset enabled the model to generalize stirrup and tie features better; the model with a smaller learning rate converged insufficiently within the same number of epochs, and the model performed reliably even when the test images were resized. Overall, the convolutional neural network-based space detection model for stirrups and ties performed with high accuracy, with the learning rate as the significant factor affecting the model's performance.

Keywords: Convolutional neural network, Dataset size, Learning rate, Image resolution, Stirrup

1. INTRODUCTION

Time, cost, and quality management should be optimized in construction project management. However, it is not easy to achieve all three criteria simultaneously, as the relationships of these criteria conflict with one another in various cases. One of these cases is the inspection of stirrups and tie spacing. Checking each spacing of stirrups and ties is tedious, especially in large-scale projects. However, when the process of checking is sped up, the quality checking for these reinforcements could be compromised, making the inspection process critical in maintaining structural integrity.

A study examined reinforced recycled coarse aggregate (RCA) concrete with different spiral stirrup configurations and RCA replacement levels, focusing on compressive strength [1]. With the same mixture proportions, increased RCA replacement levels yielded a decreased compressive strength [1]. However, the proper spiral stirrup configuration compensated for this decrease in compressive strength, which made reinforced RCA concrete structurally viable due to the stirrup confinement [1]. The reduction of stirrup spacing significantly increased the strength and ductility of the reinforced RCA concretes [1]. These results demonstrate the significant effect of proper stirrup spacing on the overall strength of a reinforced concrete structure.

Another crucial type of steel reinforcement is column ties. Columns are considered important concrete members for structural strength and resilience [2]. Extensive studies on displacement and curvature ductilities have emphasized the role of confinement in enhancing column ductility. Studies show that columns with heavy transverse reinforcement and proper detailing can attain high ductility levels [2].

Regarding the application of Convolutional Neural Network, there are numerous emerging studies in civil engineering and other fields. The capability of Convolutional Neural Networks (CNNs) was demonstrated to automate the inspection of main rebars in reinforced concrete columns, achieving 94.61% accuracy [3]. In terms of detecting distances, CNN was utilized to measure person-to-person distance, achieving an accuracy of 90% within 2 meters of capture, up to 70% within 5-6 meters of capture [4].

Convolutional Neural Networks are also utilized in the maintenance of public infrastructure, specifically for pavement inspections. The limitations

of traditional, labor-intensive road inspection methods propose the need for an efficient and cost-effective inspection system [5]. Using collected pavement images from Japan National Route 4, YOLOv3 detection performance was observed. From the results, a precision value of 0.7 and an average IoU of 50.39% were achieved, demonstrating effectiveness and good accuracy in identifying pavement defects [5].

Similarly, Faster Region Convolutional Neural Network (FRCNN) was used in developing an automated damage detection system for heritage masonry structures [6]. The study resulted in a cost-effective, reliable, and high-precision system based on FRCNN, due to its automation and accuracy results [6]. The FRCNN with the ResNet152 backbone had the highest accuracy and recall, yielding 81.29% and 81.13%, respectively [6]. The results of this specific study highlight the automation capabilities, with high reliability and cost-effectiveness, of CNNs when applied in the engineering field.

Unlike existing studies that focus primarily on detecting and counting longitudinal and transverse rebars for comparison with technical drawings, this study integrates object detection with centroid-based geometric analysis to automatically determine stirrup and tie spacing. The proposed approach extends CNN-based detection beyond simple recognition into a quantitative structural assessment framework, enabling automated spacing verification for quality control purposes.

The significance of stirrups and ties in terms of structural integrity demands careful inspection. Spotting incorrectly spaced stirrups and ties without the use of measuring devices might be easy for an experienced inspector. However, the lack of quantified inspection data is subjective, leading to inconsistent and unreliable results, especially when done by a less experienced inspector. By applying recent advancements in deep-learning algorithms, specifically neural networks, to the engineering field, the tedious inspection process of stirrup and tie inspections can be further optimized and automated through data-driven methods.

In line with the tedious process of manual checking and feature extraction capabilities of Convolutional Neural Networks, this study applied CNN in detecting stirrup and tie spacing in beams and columns. Unlike other studies that have utilized CNNs for structural analysis and damage detection, this study focused on the application of neural networks in a construction inspection context. Although there are similar studies that inspect the main reinforcement bars and detect object distances using CNN, this study combined these two applications: reinforcement bar inspection and object distance detection, specifically for the inspection of transverse reinforcement spacings, including stirrup and tie spacings.

The paper is organized as follows: Section 2 presents the research significance of the study; Section 3 describes the materials and methods utilized; Section 4 discusses the results and analysis of the findings; Section 5 provides the conclusions drawn from the study; and Section 6 lists the references used.

2. RESEARCH SIGNIFICANCE

This study contributes to society by contributing to two sustainable development goals: SDG 9: Industry, Innovation, and Infrastructure and SDG 11: Sustainable Cities and Communities. It enhances infrastructure resilience and sustainability through the automation of inspection of beam stirrups and column ties, improving time efficiency and structural integrity.

Moreover, the study supports SDG 9 Target 9.5 by integrating CNN into traditional construction practices, replacing subjective and manual inspections with objective-based, data-driven verification that improves accountability and structural safety. It also supports SDG 11 Target 11.5 by helping ensure proper transverse reinforcement design, reducing the risk of structural failure during earthquakes, therefore, minimizing disaster-related casualties and economic losses.

In the engineering field, the study contributes to expanding the pool of neural network applications, specifically convolutional neural network applications, in civil engineering and construction management. The research contributes to fostering similar convolutional neural network applications in the construction management field of engineering. More specifically, construction projects could benefit from the automation of stirrup and tie spacing by optimizing quality and time aspects in the iron triangle of project management.

3. MATERIALS AND METHODS

3.1 Phase 1: Physical Stirrup/Tie Model Creation

3.1.1 Procurement of Rebar and Tie Wires

The procurement process involved purchasing reinforcing steel bars (RSB) and tie wires at a local hardware store in Metro Manila, Quezon City. The main reinforcing bars of the physical model was composed of Grade 33 12 mm diameter deformed round steel bars at 6 meters commercial length. According to the ACI code, at least a No. 3 (10 mm diameter or bigger should be used) steel bar is

required for columns with No. 10 main reinforcing bars or smaller (equivalent to 32 mm or smaller). To follow the guidelines provided by the Code, a Grade 33 10 mm diameter deformed round steel bar was used for the lateral ties. Lastly, a gauge 16 galvanized wire was utilized as tie wire for steel bar intersections and splicing joints.

3.1.2 Creation of Physical Rebar Stirrup/Tie Model

A controlled environment was set up for the creation of the physical model. The column and beam rebar model was created using the procured reinforcing steel bars and tie wires. The column rebar model conformed to 300 mm long, 200 mm wide, and 1250 mm high dimensions. The dimensions of the beam rebar model were 300 mm high, 200 wide, and 1250 mm long.

Both column and beam models had three setups with varying spacing. The physical column model featured fixed spacing, wherein the spacing of the first, second, and third setups were 90 mm, 140 mm, and 190 mm, respectively. On the other hand, the physical beam model featured variable spacing, wherein spacing at the beam ends was smaller. Table 1 summarizes the measurements of variable spacing. Also, see Fig. 1 below for the proper illustration of structural member dimensions.

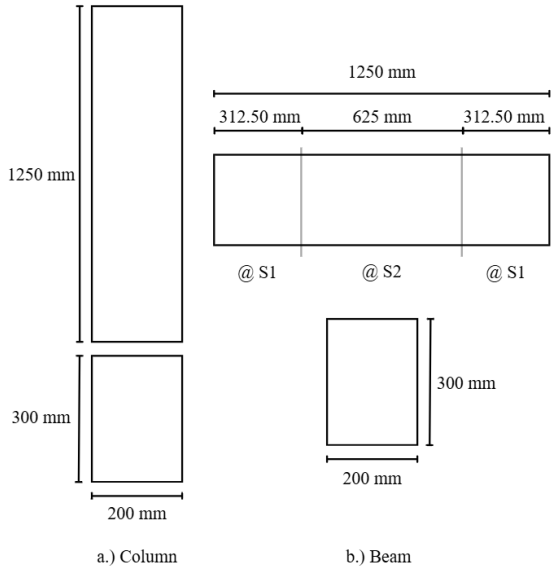

Fig. 1 Dimensions of physical model

Table 1. Variable spacing of beam physical model

Setup Number	S1	S2
1	90	140
2	140	190
3	110	190

Note: Spacings are in millimeters and measured on center

3.2 Phase 2: Dataset Generation

3.2.1 Preparation of Raw Images

The dataset was primarily obtained from the physical model setup, which featured an adjustable mechanism. The physical model was photographed under consistent lighting and background conditions. A total of 340 raw images were collected from this setup, wherein 170 images comprised both the beam and column. Furthermore, dataset splitting was done by applying a 70-15-15 split for the training, validation, and test sets. Table 1 summarizes the number of images per split classification.

Table 2. Detailed number of data per classification

Dataset Split Classification	Number of Images
Training Set	238
Validation Set	51
Test Set	51

Note: Presented number of images are pre-augmentation

3.2.2 Image Augmentation

Constructing a large dataset is crucial in effectively training the neural network model and, most importantly, achieving the best results. Furthermore, image augmentation was performed to increase the dataset size artificially and simulate environmental and background noise found in actual site conditions. Image augmentation involves adjusting the images' brightness, scale, blurring, rotation, and perspective transformation [3]. In this study, the image editing software Windows Photo and Matrix Laboratory was utilized to apply the following image augmentation techniques: rotation, salt and pepper noise, brightness, contrast, blur, saturation, hue shift, and horizontal flip. From the 238 raw images in the training set, 1904 images were generated post-augmentation. A total of 2142 images were used in training the CNN model for learning rate observation and varying image resolution. For the training of CNN model in dataset variation, three loops were performed, comprising of 714, 1428, and 2142 images, respectively.

3.3 Phase 3: CNN Model Development

3.3.1 Implementing CNN Stirrup/Tie Identification Training & Stirrup/Tie Bound Labeling

Training and testing are essential for AI model performance, and ground truth data defines the real-world reference. It is used during model training to identify features and during testing to evaluate accuracy. Generating ground truth involves accurately labeling raw data. In this study, MATLAB's

Image Labeler was used to create ground truth data by labeling regions of interest with bounding boxes, as shown in Fig. 2.

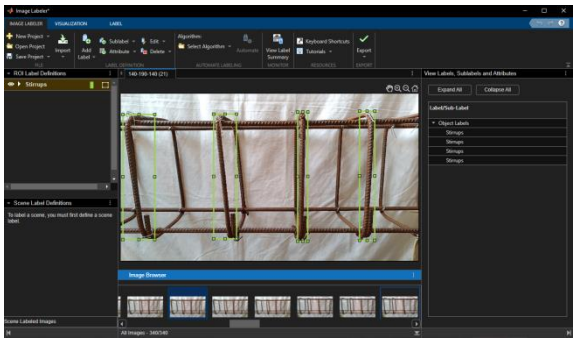

Fig. 2 Image Labeler from MATLAB software

The training network program and object detection technology used were MATLAB and YOLOv2, respectively. RCNN, Fast R- CNN, Faster R-CNN, and YOLOv2 were the detection techniques available in the MATLAB program [7]. Initially, the researchers attempted to utilize YOLOv3 due to its superior detection performance compared to the aforementioned models [8]. However, due to hardware limitations, the researchers opted for an alternative model, YOLOv2. YOLO delivers detection performance comparable to Faster R-CNN, while YOLOv2, as an improved version of YOLO, maintains this comparable accuracy with significantly higher processing speed [7]. The script used to understand the training of the object detector was indicated by the *detector* and *options* input: trainYOLOv2ObjectDetector(trainingDataDS, detector, options). The parameters utilized in the training include the sgdm optimization solver with an initial learning rate of 0.001 with constant rate schedule, a maximum of 100 epochs, a mini-batch size of 16, and 20 iterations of validation frequency.

3.3.2 Locating Object Centroids

The centroid location of beam stirrups and column ties was performed using Matrix Laboratory, using the bounding box coordinates generated in stirrup/tie identification and bound labelling, wherein each label defined the spatial extent of each identified stirrup and tie.

3.3.3 Calculation of Distance Between Stirrup/Ties

In analytic geometry, the distance between two points is the length of the line connecting them, calculated using the distance formula. In this study, the spacing between beam stirrups or column lateral ties was computed by measuring the distance between consecutive centroids obtained in Step 7.

A calibration factor (CF) was also multiplied by the determined distance value. As the distance value is in pixel units, a calibration factor (CF) helped convert the spacing value to real-world units. This was done by implementing an interactive calibration using a MATLAB function that allowed the researchers to draw a line on the test images corresponding to a known physical distance, particularly stirrup and tie spacing in the physical model. Using the known physical distance, the pixel length of the drawn line was computed, and the scale factor between pixels and millimeters was established.

3.3.4 Space Detection Model Testing

Spacing detection was tested by comparing the model's calculated values with the actual spacing of beam stirrups and column lateral ties. The comparison assessed how effectively the neural network could detect these elements. This step was critical, as high performance in spacing detection was essential to the study. Equation (1) shows the percent error formula, while Equation (2) presents the model accuracy formula.

$$Error(\%) = \frac{|detected - actual|}{actual}(100\%) \quad (1)$$

$$MA(\%) = 100 - Error(\%) \quad (2)$$

Model accuracy (MA) showed the difference in size between the model's calculated spacing and real spacing value. A lower MA value indicates inconsistencies in the spacing detection and neural network model. Conversely, a higher MA value signifies closer alignment with the actual spacing, indicating strong performance of the spacing detection model and CNN.

3.4 Phase 4: Varying Image Resolution

The visual quality of images is based on the pixel information they contain (pixels per inch), also known as image resolution. Image scaling is an augmentation technique to increase training datasets and improve image classification and detection. Image scaling was performed using Matrix Laboratory, wherein image resolution of the test set was altered. Image scaling factors used were 0.25, 0.50, 1.00, 1.50, and 2.00.

3.5 Phase 5: Learning Rate Observation

The learning rate is a key parameter affecting model efficiency and detection accuracy. A rate that's too high can cause instability, while one that's

too low can slow convergence. Therefore, selecting an appropriate value is essential for fast, stable optimization.

In this study, MATLAB's *trainingOptions* function was used to adjust the *InitialLearnRate*, with values of 0.001, 0.0001, and 0.00001. The authors' computational resources were limited by hardware capacity, with only three learning rates being tested in the study

3.6 Phase 6: Evaluating the CNN Model

To analyze the relationship between CNN accuracy and dataset size, learning rate, and image resolution, multiple regression analysis was performed using Microsoft Excel. Accuracy and average precision was the dependent variable, while dataset size, learning rate, and image resolution were the independent variables. P-values were used to assess statistical significance, and ANOVA tested the model's fit.

$$y = b_1x_1 + b_2x_2 + \ldots + b_nx_n + c \quad (3)$$

The final output of the study was the CNN model's space detection accuracy based on varying dataset sizes, reduced pixel information, and changes on learning rates, providing guidance for for engineers and designers in practical inspection and decision-making.

4. RESULTS AND DISCUSSION

4.1 Location Detection vs. Dataset Size

Table 2 shows a consistent improvement in the model's average precision (AP) as the dataset size increased from 714 to 2142 training images. This upward trend indicates that a larger dataset enabled the model to better generalize stirrup and tie features, reducing overfitting.

Table 3. Average location detection precision due to dataset size variation

Number of Training Images	Average Precision
714	0.56
1428	0.71
2142	0.75

With 714 training images, the AP was relatively low at 0.55, suggesting that the model lacked sufficient images to learn feature point variations in the dataset. As the number of training images doubled to 1428, the AP increased to 0.71, reflecting the positive impact of additional image diversity on feature learning. The highest AP of 0.75 was attained with 2142 training images, signifying that the model benefited from more exposure to distinct feature patterns and orientations.

Figure 3 shows the number of detected ties for test image 16, labeled as red rectangles.

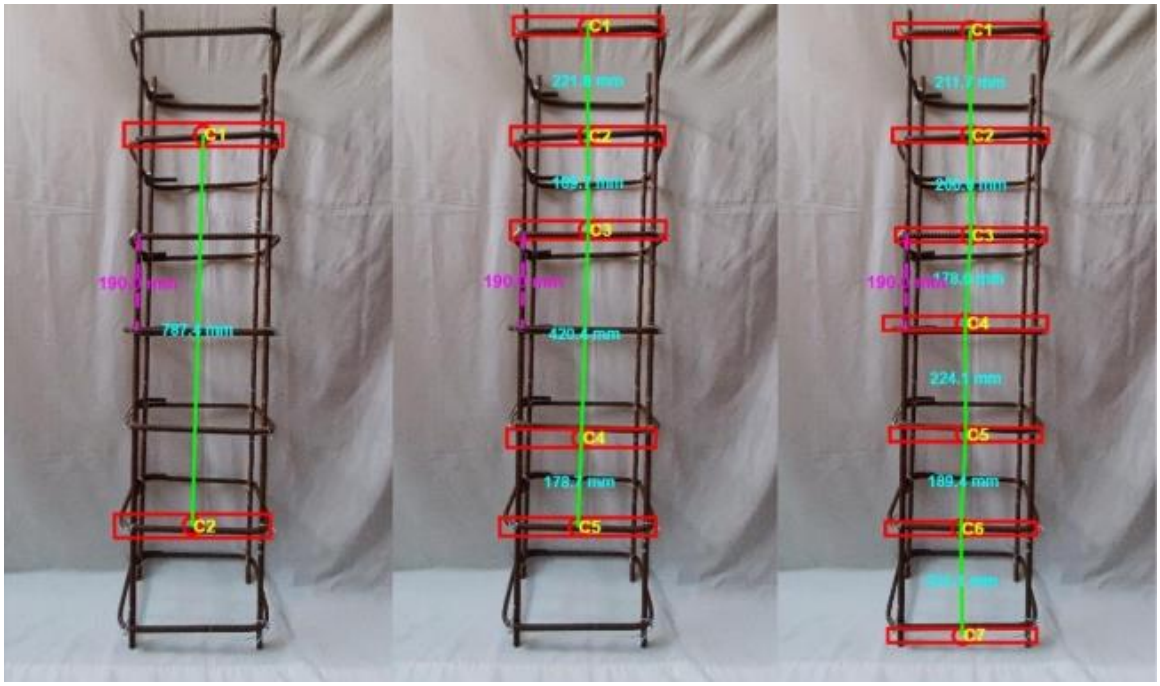

Fig. 3 Test image 16 for dataset size 714, 1428, and 2142 image

In the left image, it can be observed that there are only two red rectangles, indicating that the model trained with 714 images struggled to detect all tie locations due to limited exposure to diverse feature patterns.

In contrast, the middle image (1428 training images) demonstrated a noticeable improvement, with more tie locations correctly detected, suggesting that the model learned a wider range of visual detection. Finally, the right image (2142 training images) exhibited the most accurate detection, with all tie locations correctly detected.

4.2 Location Detection vs. Learning Rate

Figure 4 illustrates the model's detection performance with stirrups under various learning rates. In the top-most image (learning rate = 0.001), the model accurately detects all stirrups. In the middle image (learning rate = 0.0001), fewer stirrups are detected, and some bounding boxes appear out of position. This reduction in location detection suggests that the model's learning progress slowed down due to the lower value of learning rate.

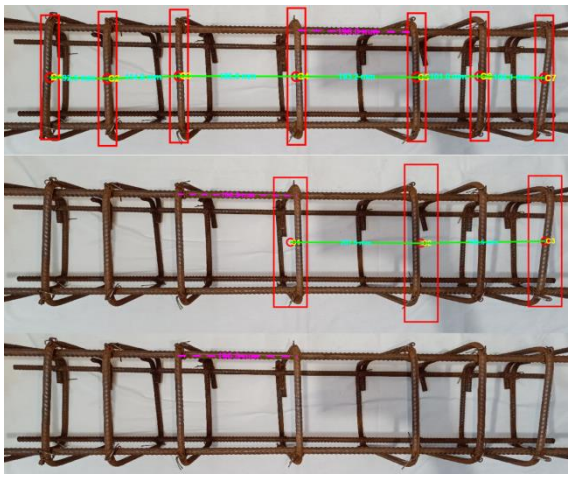

Fig. 4 Test image 9 for learn rate 0.001, 0.0001, and 0.00001

Finally, the bottom image (learning rate = 0.00001), the model fails to identify any stirrups. This reflects severe underfitting due to excessively small value of the learning rate, which limited the model from learning meaningful features and patterns from the training data.

4.3 Location Detection vs. Image Resolution

Figure 5 presents the model's detection performance with stirrups under various scale factors. In the top-most image (0.25 scale factor), the model accurately detects five stirrups, as shown by the clearly defined red rectangles along the beam. In the middle image (1.00 scale factor), additional stirrups are detected, increasing the total number of correct detections to seven. This increase in location detection suggests that the scale factor affects the model performance due to the lower detail quality in the said test image. Finally, the bottom image (2.00 scale factor), the model accurately detected the same number of stirrups as 1.00 scale factor. However, bounding boxes in the bottom image were more correctly positioned, possibly contributing to higher spacing detection accuracy. This indicates that the model performed slightly better with higher resolution images, likely due to clearer visual features and sharper edge details that enhanced feature representation.

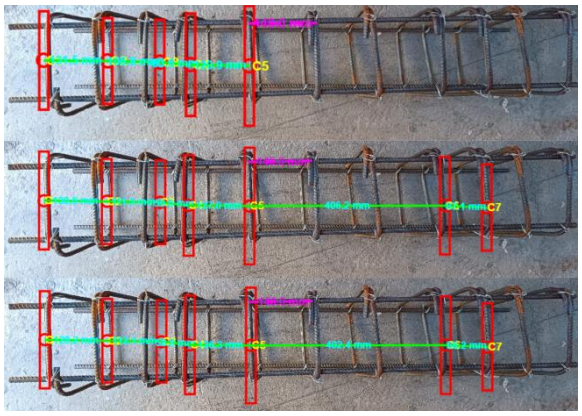

Fig. 5 Test image 19 for scale factor 0.25, 1.00, and 2.00

Regarding the acceptability of the obtained average precision (AP) values in stirrup and tie location detection, various studies support the findings presented in this paper. For instance, YOLOv2 was utilized in bridge surface defect detection and achieved AP values ranging from 0.78 to 0.87 [9], which align closely with the performance range observed in this study. Similarly, YOLOv2 architecture was utilized for leukocyte (considered a small object) detection and classification, reported an AP of 0.62 [10]. Additionally, Faster R-CNN was evaluated for small object detection tasks and reported an AP of 0.65 [11].

These studies demonstrate that achieving AP values within 0.60-0.80 range is typical for object detection models dealing with complex image conditions and structural details. Moreover, these studies reinforce the validity of the study's AP findings, confirming that the model's location detection for stirrup and tie falls within a credible and established performance range for similar deep

learning-based detection systems.

4.4 Multiple Regression Analysis

Data analysis in Microsoft Excel's Analysis ToolPak was used to implement multiple linear regression analysis for each independent variable in this study: average precision of stirrup/tie location detection and average accuracy of stirrup/tie spacing detection. The dependent variables were the dataset size expressed as the number of training images, the learning rate initialized in the *InitialLearnRate* function, and image resolution expressed as scale factors.

4.4.1 Location Detection Performance

For the stirrup/tie location detection performance of the CNN model, the multiple linear regression analysis yielded a correlation coefficient of 0.9005 (R = 0.9005) and a coefficient of determination of 0.7298 (Adjusted R-squared = 0.7298). A correlation coefficient of 0.9005 indicates a strong positive linear relationship between the dependent variable and the independent variable [12]. This interpretation further suggests that dataset size, learning rate, and image resolution strongly affect the average precision of the stirrup/tie location detection.

$$AP=0.0116S+506.4193L+0.0001N-0.0232 \quad (4)$$

The variables *S*, *L,* and *N* represent scale factor, learning rate, and number of training images, respectively. In observance of the algebraic signs of the coefficients for the dependent variables, all of them have a positive coefficient, which supports the direct relationship between the dependent variables and the average precision of the detection. Mathematically, the increase in the variables S, L, and N leads to the increase in the variable y, representing the average precision of the model's location detection.

Figure 6 below visualizes the influence of the number of training images on the model's average precision in stirrup/tie location detection. As is visible in the data's trendline, the trendline's nature is nearly flat, which indicates that the dataset size expressed as the number of training images has little to no influence on the CNN model's average precision in stirrup/tie location detection. Furthermore, the R-squared value of 0.0054 is near zero, indicating little to no explanatory power of the dataset size variations on the model's average precision in stirrup/tie location detection.

On the other hand, Figure 7 visualizes the influence of learning rates on the model's average precision in stirrup/tie location detection. Contrary to Fig. 6, the learning rate data show an observable, fairly positively sloped line, indicating a strong influence of learning rates on the CNN model's capability to locate stirrup/tie, as measured by average precision. Learning rates and the model's average precision are directly related.

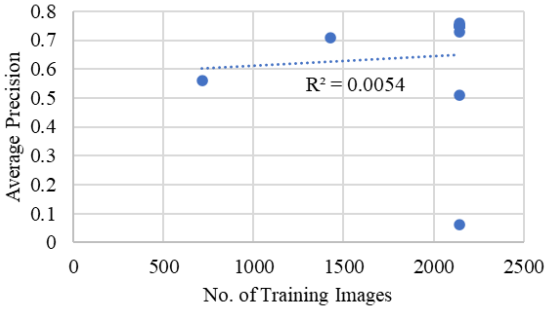

Fig. 6 Average precision of dataset size variations

The correlation suggests the model failed to generalize well due to an excessively low learning rate, leading to unreliable detections. As a limitation of the study, the maximum number of epochs was set to 100 to properly analyze the effect of learning rates alone on the model's accuracy and precision, which contributed to the correlation between learning rates. This observation is further supported by the R-squared value of 0.7432, which indicates that most of the variations in the observed average precision in stirrup/tie location detection are explained by the learning rate.

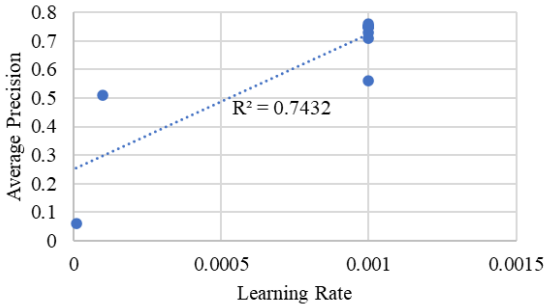

Fig. 7 Average precision of learning rate variations

A similar observation to the dataset size visualization is observed in Figure 8, which shows the influence of image resolution expressed in scale factors. The trendline is also nearly flat, indicating that image resolution has little to no influence on the

CNN model's average precision in stirrup/tie detection.

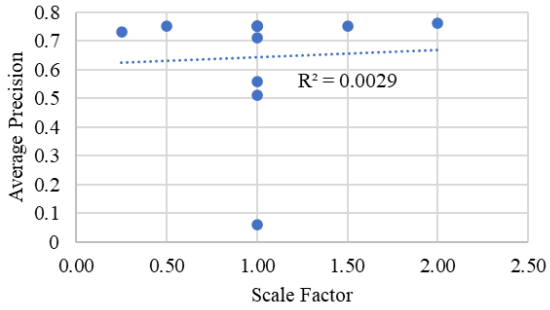

Fig. 8 Average precision of image resolution variations

The R-squared value of 0.0029 shows low explanatory power for the variances in average precision of stirrup/tie location detection. The regression lines for Fig. 6, Fig. 7, and Fig. 8 are positively sloped, indicating a direct relationship with average precision and supporting the earlier qualitative observations. However, the R-squared values indicate that only the learning rate shows a strong relationship; therefore, the learning rate is the only independent variable that strongly influences the model's average precision.

The one-way ANOVA yielded a significance-F of 0.0063. Since the significance F is lower than the alpha value (α = 0.05), it is concluded that the null hypothesis that there is no significant relationship between the average precision of stirrup/tie location detection and that of dataset size, learning rate, and image resolution is to be rejected. Therefore, the results of the one-way ANOVA lean towards the alternative hypothesis that there is a significant relationship between the average precision of stirrup/tie location detection and that of dataset size, learning rate, and image resolution.

For the dataset size, a p-value of 0.1603 was the output of the one-way ANOVA, which is greater than the alpha value (α = 0.05), indicating that dataset size does not have a significant relationship to the average precision of stirrup/tie location detection. This finding is in accordance with the result of a study [13], which also concludes that the increase in dataset size does not significantly affect the performance of machine learning models. The finding of a p-value of 0.2965 further extends the conclusion that dataset size is not a significantly influential factor in object detection for convolutional neural network models.

For the learning rates, the one-way ANOVA yielded a p-value of 0.0010, less than the alpha value (α = 0.05), indicating that learning rates have a significant relationship to the average precision astirrup/tie location detection. This significant effect of learning rates on the average precision of stirrup/tie detection finding is aligned to the statement in a deep neural network study [14], that learning rate is one of the most prominent parameters where the sensitivity of deep neural networks is observed. Furthermore, learning rates have a significant impact, as they can control a neural network model's performance [14].

For the image resolution, a similar finding to the dataset size, that there is no significant relationship between the average precision of the model's stirrup/tie location detection, was indicated by the p-value of 0.8836, greater than the alpha value (α = 0.05). This finding implies that the usage of image augmentation techniques proved to be effective in training the CNN model to different image conditions. Even though image scaling was not implemented in the training set images, the CNN model performed well in scaled test images. The study that deep learning models trained on augmented images performed better than models trained on raw datasets supports this finding of no significant relationship of image resolution variations in test images to the average precision of stirrup/tie location detection [3].

4.4.2 Spacing Detection Performance

The stirrup/tie spacing detection showed similar results to the stirrup/tie location detection, which is expected, as the spacing detection depends on the model's stirrup/tie location detection performance. The multiple regression analysis yielded a correlation coefficient (R) of 0.9235. The correlation coefficient (R) of 0.9235 falls in the same range in the interpretation table from a study [15], indicating a strong positive linear relationship between the dependent variables and the independent variable. Additionally, the multiple regression analysis yielded a slightly higher coefficient of determination (Adjusted R-squared) of 0.7898. Even though not all variations of the average accuracy are explained by the regression, the value of the coefficient of determination is justified for the same reason in the multiple regression of the stirrup/tie location detection. Some parameters are learned in the neural network's training, which introduces noise to the location detection, thus also introduces noise to the spacing detection [15]. The multiple regression between the average accuracy of spacing detected and the dependent variables is shown in the

equation below.

$$MA=0.0618S+2082.8345L-0.0002N+90.4408 \quad (5)$$

Similar to Eq. (4), the learning rate has the highest coefficient magnitude, indicating the strongest influence among the dependent variables, and it is by a large margin. In observance of the algebraic signs of the coefficients, two out of three have a positive sign, which supports the positive relationship interpretation of the correlation coefficient (R).

Figure 9 below plots dataset size variations and their corresponding average accuracy in stirrup/tie spacing detection. The points of the dataset variations have a negative-sloped trendline, which implies an indirect relationship between the number of training images and the average accuracy in stirrup/tie spacing detection.

This implication is the same as the significance of the negative coefficient in the regression line equation. However, it is notable that it has an R-squared value of 0.0834, close to zero. This close-to-zero R-squared implies a very low relationship strength, as it only explains 8.34% of the variance of the average accuracy in stirrup/tie spacing detection.

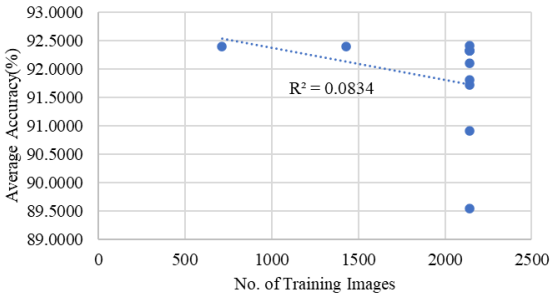

Fig. 9 Average accuracy of dataset size variations

Figure 10 plots learning rate variations and their corresponding average accuracy in stirrup/tie spacing detection, showing a similar nature of the trendline to that of Figure 9. Figure 10 shows a positive trendline for the learning rate variation data points, indicating a direct relationship. This direct relationship further supports that the model failed to generalize well due to an excessively low learning rate, leading to unreliable detections.

An R-squared of 0.8419 indicates that the learning rate explains 84.19% of the average stirrup/tie spacing detection accuracy. This high R-squared indicates a high relationship strength of learning rate and average accuracy in spacing detection This similarity is to be expected as the spacing detection relies on the location detection.

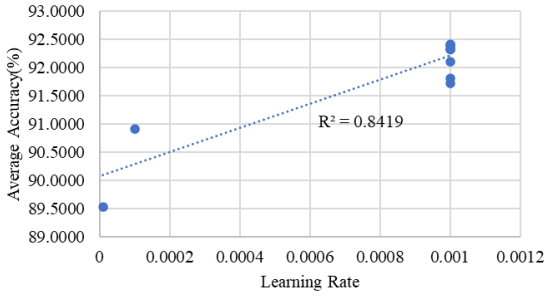

Fig. 10 Average accuracy of learning rate variations

Lastly, Figure 11 plots the image resolution variations and their corresponding. Figure 11 shows a near-flat, positively sloped trendline for the image resolution data points. The nature of the trendline indicates a low relationship strength. Similarly, the R-squared values showed that only the learning rate has a strong relationship, indicating a strong influence on the model's average accuracy. The slopes of Fig. 9, Fig. 10, and Fig. 11, specifically Fig. 9, are different from those of Fig. 6, Fig. 7, and Fig. 8. However, these do not contradict the earlier qualitative observations since the observations were mainly about the number of detected stirrups/ties, while Fig. 9, Fig. 10, and Fig. 11 are about the measured spacing by the model compared to its actual spacing.

The R-squared value of 0.0026 implies that only 0.26% of the image resolution variations explains the average accuracy of stirrup/tie spacing detection, supporting the low relationship strength between image resolution and average stirrup/tie spacing detection accuracy. This low relationship strength indicates low influence of image resolution on the model's performance in spacing detection.

Similarly, the R-squared values showed that only the learning rate has a strong relationship, indicating a strong influence on the model's average accuracy. The slopes of Fig. 9, Fig. 10, and Fig. 11, specifically Fig. 9, are different from those of Fig. 6, Fig. 7, and Fig. 8. However, these do not contradict the earlier qualitative observations since the observations were mainly about the number of detected stirrups/ties, while Fig. 9, Fig. 10, and Fig. 11 are about the measured spacing by the model compared to its actual spacing.

The one-way ANOVA yielded a significance-F of 0.0027. This significance-F is less than the alpha value (α = 0.05), indicating rejection of the null hypothesis. This rejection suggests a significant

relationship between the dataset size, learning rate, image resolution, and the average stirrup/tie spacing detection accuracy.

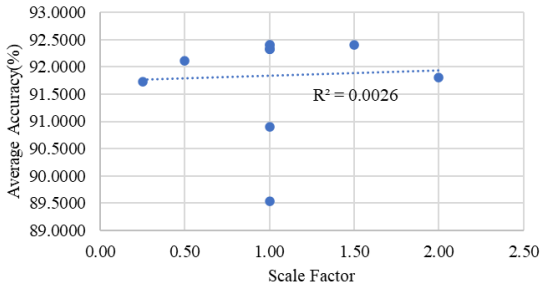

Fig. 11 Average accuracy of image resolution variations

Furthermore, the p-values for the number of training images, learning rate, and scale factor were 0.5096, 0.0005, and 0.8345. From these p-values, the learning rate was the only p-value less than the alpha value ($\alpha = 0.05$), indicating that the learning rate is the only dependent variable with a significant relationship to the average stirrup/tie spacing detection accuracy.

Since the model's spacing detection relies on the model's location detection, the same reasons apply as to why the learning rate was the only dependent variable that significantly influences the average accuracy of stirrup/tie location detection.

5. CONCLUSION

Average precision (AP) for location detection improved consistently with increasing dataset size, reaching the highest AP of 0.75 with 2142 training images, indicating better generalization and reduced overfitting due to more exposure to distinct feature patterns and orientations.

In terms of learning rate, performance decreased as the learning rate decreased with 0.001 achieving the highest AP by balancing stable convergence and efficient learning, whereas very low learning rates resulted in slow convergence, ineffective parameter updates, and underfitting.

For image resolution, AP showed a slight upward trend with higher scale factors. The performance reached its best at 0.76 for a scale factor of 1.50, followed by 0.76 at 2.00, suggesting that higher resolution improved clarity and edge definition, therefore enhancing feature extraction.

The correlation coefficients (0.9005 and 0.9235) and significance-F values (0.0063 and 0.0027) indicate a strong positive linear and statistically significant relationship between the dataset size, learning rate, and image resolution, and the model's stirrup/tie detection. The p-values for both stirrup/tie location detection and spacing detection imply that only the learning rate has a significant relationship and influence on the model's performance.

6. RECOMMENDATIONS

Developing a method to properly label angled images is recommended to enhance feature recognition of stirrups and ties.

Explore the integration of the spacing detection model into a mobile application to enable real-time, on-site checking of stirrup and tie spacing.

7. REFERENCES

[1] Pham T. T., Nguyen K.H., and Nguyen T. T., Compressive Strength of Confined Reinforced Recycled Coarse Aggregate Concrete Columns, International Journal of GEOMATE, Vol. 29, Issue 136, 2025, pp. 69–77.

[2] Soehardjono A., Sabariman B., Wisnumurti, and Wibowo A., Contribution of Steel Fibers on Ductility of Confined Concrete Columns, International Journal of GEOMATE, Vol. 23, Issue 97, 2022, pp. 188–195.

[3] Wang S., Kim M., Hae H., Cao M., and Kim J., The Development of a Rebar-Counting Model for Reinforced Concrete Columns Using an Unmanned Aerial Vehicle and Deep-Learning Approach, Journal of the Construction Division and Management, Vol. 149, Issue 11, 2023, pp. 1-13.

[4] Tsai Y., Modales A. V., and Lin H., A Convolutional Neural-Network-Based Training Model to Estimate Actual Distance of Persons in Continuous Images, Sensors, Vol. 22, Issue 15, 2022, Article 5743

[5] Opara J. N., Thein A. B. B., Izumi S., Yasuhara H., and Chun P.-J., Defect Detection on Asphalt Pavement by Deep Learning, International Journal of GEOMATE, Vol. 21, Issue 83, 2021, pp. 87–94.

[6] Thansirichaisree P., Klincharoen O., Buatik A., Potipipit S., and Poovarodom N., Damage Detection in Historical Structures Using Faster Region-Based Convolutional Neural Network, International Journal of GEOMATE, Vol. 29, Issue 132, 2025, pp. 172–181.

[7] Kim T., Hong S., and Choo S., Algorithm of Smart Building Supervision for Detecting and Counting Column Ties Using Deep Learning, Applied Sciences, Vol. 12, Issue 11, 2022, Article 5535.

[8] Bhatlawande S., Shilaskar S., Anantwar V., and Avhad L., Integrated System for Vision-Based SLAM Implementation and Object Detection using AKAZE Feature Descriptor, International Conference on Computational Intelligence and Sustainable Engineering Solutions, 2023.

[9] Teng S., Liu Z., and Li X., Improved YOLOV3-Based Bridge Surface Defect Detection by Combining High- and Low-Resolution Feature Images, Buildings, Vol. 12, Issue 8, 2022.

[10] Abas S. M., Abdulazeez A. M., and Zeebaree D. Q., A YOLO and Convolutional Neural Network for the Detection and Classification of Leukocytes in Leukemia, Indonesian Journal of Electrical Engineering and Computer Science, Vol. 25, Issue 1, 2022, pp. 200-213.

[11] Mazen F. M. A. and Shaker Y., Small Object Detection in Complex Images: Evaluation of Faster R-CNN and Slicing Aided Hyper Inference, International Journal of Advanced Computer Science and Applications, Vol. 16, Issue 3, 2025, pp. 951-960.

[12] Ahmed M. H., Kutsuzawa K., and Hayashibe M., Transhumeral Arm Reaching Motion Prediction through Deep Reinforcement Learning-Based Synthetic Motion Cloning, Biomimetics, Vol. 8, Issue 4, 2023, Article 367.

[13] Bailly A., Blanc C., Francis É., Guillotin T., Jamal F., Wakim B., and Roy P., Effects of Dataset Size and Interactions on the Prediction Performance of Logistic Regression and Deep Learning Models, Computer Methods and Programs in Biomedicine, Vol. 213, 2021.

[14] Al-Khamees H. A. A. A., Al-A'araji N., and Al-Shamery E. S., Enhancing the Stability of the Deep Neural Network Using a Non-Constant Learning Rate for Data Stream, International Journal of Electrical and Computer Engineering, Vol. 13, Issue 2, 2023, pp. 2123–2130.

[15] Hammad, M. M., Artificial Neural Network and Deep Learning: Fundamentals and Theory, Egypt, 2024, pp.1-5